Experimental investigation of the wake behind a cooled cylinder

Jaroslav Pulec[1*], *Petra* Dančová[1], and *Václav* Vinš[2]
[1]Technical University of Liberec, Studentská 2, 460 01 Liberec Czech Republic
[2]Institute of Thermomechanics of the Czech Academy of Sciences, Dolejškova 5, 182 00 Prague Czech Republic

Abstract. An experimental channel intended for investigation of a wake behind a cooled cylinder was designed and constructed in this work. The setup is designed for measurements with air at low Reynolds numbers. The measuring techniques based on the standard visualization with a fog generator and the constant temperature anemometry (CTA) were used. The flow performance was investigated behind two cylinders placed inside a channel with square cross section. One cylinder was kept at a constant flow temperature, while the second cylinder could be cooled using a water circuit with a thermostatic bath. The dependency of the Strouhal number on the Reynolds number was evaluated and compared to the literature data and the empirical correlations. The concept of an effective temperature in a non-isothermal flow was also applied. Unfortunately, a considerable difference between the preliminary measurements and the literature data was detected. The air-flow was found to have unsatisfactory high turbulence intensity. Consequently, some modifications of the current channel design are proposed.

1 Introduction

An effect of a boundary layer separation in a case of non-isothermal flow was described by many authors [1]. The purpose of this work was to develop an experimental apparatus in the laboratory of the Technical University of Liberec enabling observation and measurement with good accuracy. The presented results were obtained as part of the master's degree thesis of the corresponding author J. Pulec [2]. The theoretical backgrounds and technical solutions were inspired mostly by the work by Trávníček et al. [3].

Reynolds number is an important characteristic number in the case of flow around cylinder. It is ratio of frictional and resistance forces. Reynolds number is defined as:

$$\mathrm{Re} = \frac{U \cdot D}{\nu_\infty}, \tag{1}$$

where U (m · s^{-1}) is a free-stream velocity, D (m) is a cylinder diameter and ν_∞ (m^2 · s^{-1}) is a kinematic viscosity related to a free-stream temperature T_∞. Due to a cylinder cooling the free-stream temperature is different from a cylinder wall temperature T_w. Heat transfer between the cooled cylinder and the air causes local temperature drop connected with variation of the kinematic viscosity and the Reynolds number.

Kinematic viscosity ν is given by the following relationship:

$$\nu = \frac{\mu}{\rho}, \tag{2}$$

where ρ (kg · m^{-3}) is the fluid density and μ denotes the dynamic viscosity (Pa · s).

In connection with the above-mentioned changes of the Reynolds number a concept of effective temperature was established [4-7]. Based on this, effective Reynolds number was defined:

$$\mathrm{Re}_\mathrm{eff} = \frac{U \cdot D}{\nu_\mathrm{eff}}, \tag{3}$$

where ν_eff (m^2 · s^{-1}) is an effective kinematic viscosity that is related to an effective temperature T_eff. The effective temperature can be evaluated from an empirical correlation determined experimentally. It is described by following relationship:

$$T_\mathrm{eff} = T_\infty + \mathrm{c}_\mathrm{eff}(T_\mathrm{w} - T_\infty), \tag{4}$$

where $\mathrm{c}_\mathrm{eff} = 0.28$ is an empirical coefficient. Critical value of effective Reynolds number $\mathrm{Re}_\mathrm{C,eff}$ was detected as $\mathrm{Re}_\mathrm{C,eff} = 47.5 \pm 0.7$ [6]. Further, an empirical relationship between the Strouhal number St and the effective Reynolds number Re_eff for heated and unheated cylinders was found [6]:

$$\mathrm{St} = 0.266 - \frac{1.016}{\sqrt{\mathrm{Re}_\mathrm{eff}}}, \tag{5}$$

The Strouhal number is defined as follows:

$$\mathrm{St} = \frac{f \cdot D}{U}. \tag{6}$$

In equation (6), f (Hz) denotes the vortex shedding frequency.

* Corresponding author: jaroslav.pulec@tul.cz

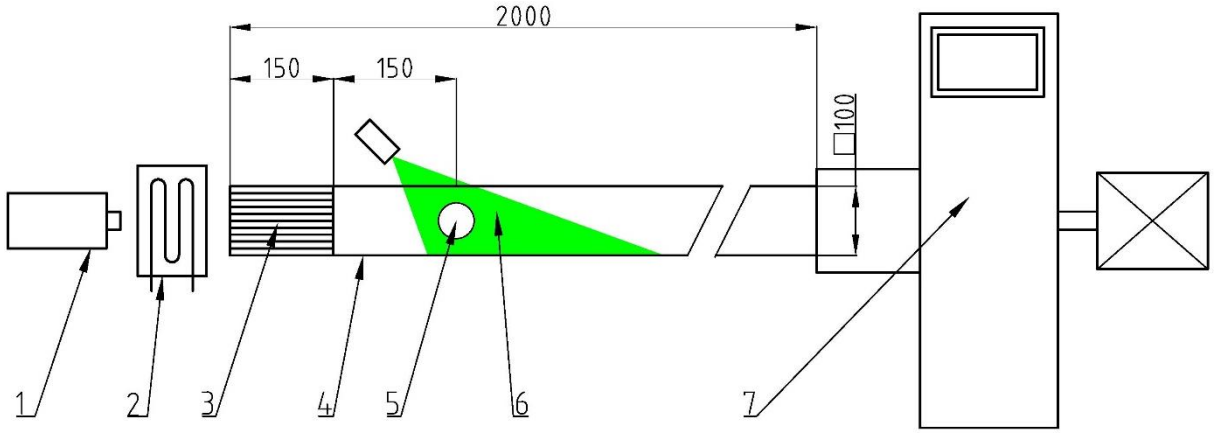

Fig. 1. Experimental apparatus. *1 fog* generator, *2* heater, *3* honeycomb, *4* experimental channel, *5* experimental area, *6* laser sheet, *7* radial fan and electric motor.

A dimensionless temperature (referred also as the temperature ratio) T^* is often used to describe the temperature situation of the non-isothermal flow. It is defined as:

$$T^* = \frac{T_\mathrm{W}}{T_\infty}. \tag{7}$$

We note that for $T^* = 1$, the flow becomes isothermal as $T_\mathrm{w} = T_\infty$.

Empirical dependence of free-stream kinematic viscosity was found by Goldstein and Cho [8]. It is described by follow equation:

$$\nu_\infty = 0.1556 \left(\frac{T_\infty}{298.16}\right)^{1.7774} \left(\frac{1.013 \cdot 10^5}{p_\mathrm{atm}}\right) \cdot 10^{-4}, \tag{8}$$

where p_atm (Pa) is atmospheric pressure.

A relationship for theoretical flow velocity can be deduced from equations (3) to (8) in the following manner [3]:

$$U = \frac{1}{4}\left[-\frac{E^*}{D^*}\cdot\sqrt{\frac{\nu_\infty(0.72+0.28T^*)^{1.7774}}{D}} + \sqrt{\left(\frac{E^*}{D^*}\right)^2 \frac{\nu_\infty(0.72+0.28T^*)^{1.7774}}{D} + \frac{}{4\left(\frac{fD}{D^*}\right)}}\right]^2, \tag{9}$$

where $E^* = -1.016$ and $D^* = 0.266$ are empirical constants [3].

Since $\nu \sim T^{1.7774}$ (8), the ratio of the Reynolds number and the effective Reynolds number can be written as follow [7]:

$$\frac{\mathrm{Re}}{\mathrm{Re}_\mathrm{eff}} = \frac{\nu_\mathrm{eff}}{\nu_\infty} = \left(\frac{T_\mathrm{eff}}{T_\infty}\right)^{1.7774}. \tag{10}$$

Using equations (4) and (10), equation (5) can be modified as follows [3]:

$$\mathrm{St} = 0.266 - \frac{1.016}{\sqrt{\mathrm{Re}}}(0.72 + 0.28T^*)^{0.8887}, \tag{11}$$

which represents an empirical definition of the Strouhal number for a non-isothermal flow around a cylinder.

2 Experimental apparatus

A simplified scheme of the experimental apparatus is shown in Fig. 1. A radial fan was used for generation and regulation of air flow in our experiment. It was driven by 2.2 kW induction motor Siemens with frequency changer enabling smooth variation of speed up to 2800 rpm.

Measurement and visualization were conducted in a measuring channel in the way of minimization of disturbances. For easier attainment of steady flow, the air channel was conceived as sucking, so a channel outlet is connected to a fan inlet. The crossing was realized by an acrylic sheet with the periodically drilled apertures for throttling the flow. The channel was 2000 mm long and had a square cross-section 100 x 100 mm. The channel was made of adhesive-bonded acrylic sheets. Temperature endurance of the sheets is 343 K for long-term application, and it softens at 373 K. Bottom and back walls were black colored for the visualization purposes. The channel inlet was created by a plastic honeycomb for a flow smoothing.

In order to achieve higher temperature difference between the cylinder and the airflow, an air heater was placed before the channel inlet. It was a 2 kW heating coil with sheet-metal case, which allowed for a constant flow temperature of around $T_\infty = 310$ K.

A measuring area with observed bodies was located 300 mm from the channel inlet as an unadvisable vorticity was found to form at a longer distance. The observed bodies, i.e. the cylinders, were made of a brass pipe with outer diameter of 2 mm. For the effective comparison of the character of the wake in the cases of isothermal and non-isothermal flow, two cylinders were used. Their orientation in the measuring area is depicted in Fig. 2 and

Fig. 4. The upper cylinder was connected to a thermostatic bath Julabo F 34-MA capable to hold a constant temperature of a coolant with a stability of ± 0.02 K. The lower cylinder was left at the free-stream temperature.

3 Experimental methods

3.1. Temperature measurement

Dewetron DEWE-5000 with software Dewesoft 6.6.7 was used for a temperature measurement. The data acquisition system allows for recording and plotting of the temperature variation over time. Six K-type thermocouples were placed inside the channel and measured the free-stream temperature T_∞. Positions of the thermocouples are shown in Fig. 2.

3.2 Visualization

The flow was visualized by fog generator Safex S2010. It was situated before the air heater. Stream of fog was sucked into the channel. The fog particles were illuminated by a laser sheet created by a pulse laser with a cylindrical lens located inside the measuring area. The laser beam had a wavelength of 532 nm. Scheme of the measuring area with the laser sheet in Fig. 2.

Visual data was recorded by a high-frequency camera Dantex Dynamic Nanosense MkIII with Nikon lens. It was able to make a film with a frame-frequency up to 15 kHz.

For setting the record parameters, the software Motion Studio 2.13 by IDT vision was used. Frequency of 300 Hz and resolution of 1280 × 644 px were employed.

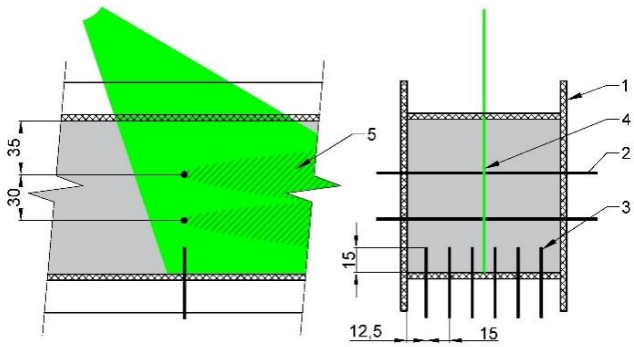

Fig. 2. Measuring area for visualization. *1* channel wall, *2* cylinders placed within the flow, *3* thermocouples, *4* laser sheet, *5* vortex structures illuminated by the laser sheet.

3.3 Velocity measurement

Velocity measurement was performed using a constant temperature anemometry (CTA) by hot-wire sensor (HWA mode). In Fig. 3, location of the velocity sensor is shown. The velocity measurement was carried out without a presence of the cylinders. The airflow was heated to adjust conditions similar to visualization and frequency measurements. According to the coordinate system in Fig. 3, the end of the sensor was traversed in the *y*-axis direction with 5 mm steps in the interval $y = (15 \div 75)$ mm. *x*-axis location was fixed at $x = 15$ mm.

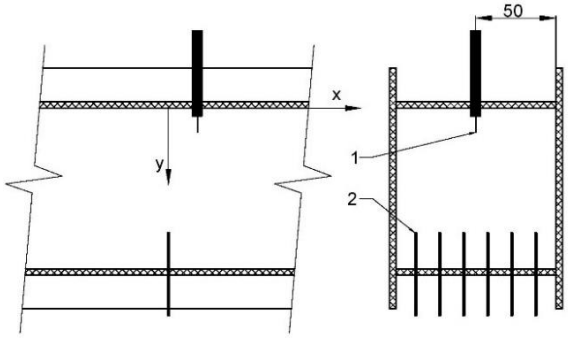

Fig. 3. Measuring area for velocity measurement. *1* sensor HWA, *2* thermocouples.

3.4 Vortex shedding frequency measurement

Two independent methods of frequency measurement were used. The first method was a frequency determination from the video, the other one was fast Fourier transform (FFT) of measured data by CTA. Both methods were used separately in different times and under slightly different conditions. Therefore, the results cannot be directly compared to each other.

HWA sensor location for the frequency determination is shown in Fig. 4. The coordinate system is the same as in Fig. 3. Sensors' coordinate locations were $x = 15$ mm, $y = 35$ mm and $y = 65$ mm for option A and option B, respectively. Frequency measurement was not conducted simultaneously but in the independent measurements, each for a period of 13 seconds.

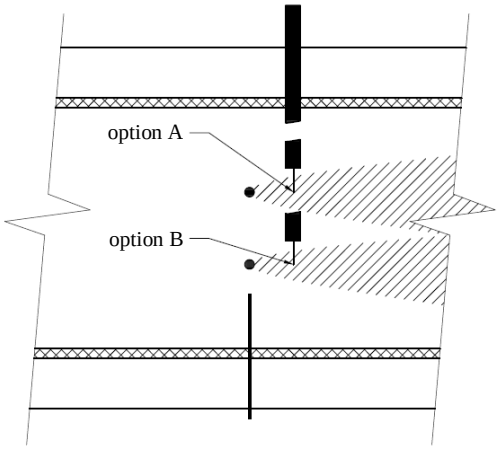

Fig. 4. Measuring area for frequency measurement. *Option A* measurement behind the cooled cylinder, *option B* measurement behind the reference cylinder.

4 Results

4.1 Visualization

All following experiments were performed at a constant rotational speed of the induction motor. At first, the cylinder connected to the cooling loop was left at the flow temperature, i.e. $T_W = T_\infty$, and afterwards the temperature was varied to $T_W = 301.1$ K, $T_W = 291.1$ K and

T_W = 281.1 K. Due to low frequency differences, the boundary cases are discussed further.

In Fig. 5 there are two pictures. Both of von Kármán vortex streets were generated in an isothermal flow. Time step between the pictures was 0.09 s approximately. Yellow vertical lines intersect the same couple of vortices. Apparently, the vortex streets have the similar proportions; it means vortex shedding frequencies and width of wakes.

Fig. 6 shows comparison of an isothermal and non-isothermal wakes. Upper vortex street represents a wake behind the cylinder cooled to T_w = 281 K, the lower cylinder is uncooled. In the non-isothermal case, the higher vortex shedding frequency and the greater width of wake can clearly be observed.

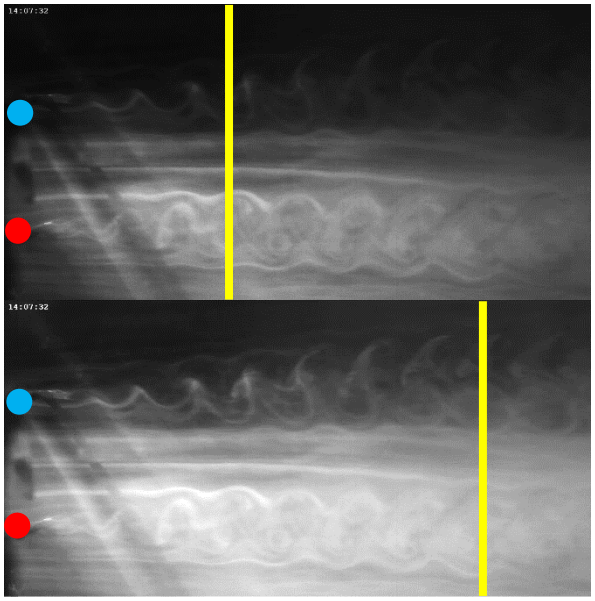

Fig. 5. Von Kármán vortex street for an isothermal case at two-time frames shifted by approximately 0.09 s. *Upper blue point* cooled cylinder (in this case, the cooling was switched off), *lower red point* reference cylinder.

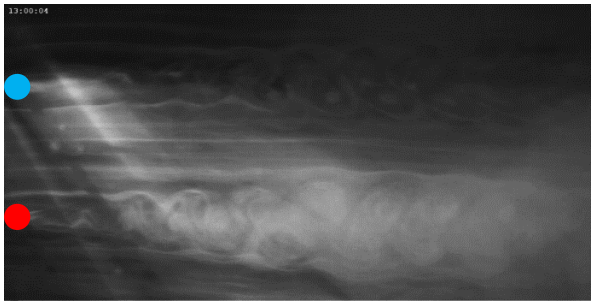

Fig. 6. Von Kármán vortex street for a non-isothermal case. *Upper blue point* cooled cylinder, *lower red point* reference cylinder.

4.2 Measured data analysis

Mean values of the flow velocity inside the channel measured at various vertical positions by the HWA sensor are shown in Fig. 7. As mentioned in chapter 3.3, y = 35 mm and y = 65 mm are the y-axis locations of the cylinders. As can be seen, the velocity profile was not uniform in the vertical direction as it varied from 0.6 to 0.66 m·s^{-1}. The velocity values were measured individually step by step. The velocity fluctuations could be caused either by an unstable fan operation or by an unsteady temperature profile within the channel.

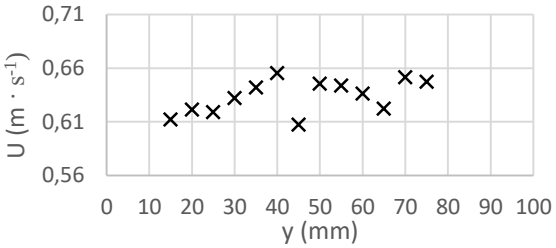

Fig. 7. Velocity profile in vertical direction.

Both measured and calculated values from the visualization experiment are summarized in Table 1. Table 2 contains data obtained from the CTA measurement. Each measurement is marked by a number and a letter. In Table 1, values on rows with the same number are evaluated from the same recording. In these cases, the conditions were identical. The upper cylinder is marked with letter *a*. Letter *b* denotes the lower reference cylinder.

From comparison of lines 1*a* and 1*b*, it is apparent that the vortex shedding frequency was approximately equal as case 1 represented an isothermal flow. Reversely when temperature ratio was decreased the frequency increased. It can also be seen that the effective Reynolds number markedly increased. Consequently, the temperature difference caused a similar effect as the increased flow velocity.

In Table 2, there are data sorted in a similar way, when a different letter marks the different time period of measurement Therefore, the thermal conditions slightly differ.

From a comparison of the free-stream viscosity, the effective viscosity, and the Reynolds numbers the change of effective values due to cooling becomes obvious. Frequencies of cooled and uncooled cylinders can be compared only partly since the measurement of wake behind cylinder *a* and cylinder *b* were made under different conditions of free-stream and the velocity also varied as shown in the CTA results. Ideally, a decrease in effective viscosity should cause a frequency increase. Due to inaccuracies in the flow temperature and the velocity distribution, the frequency change was difficult to evaluate accurately.

Graphs in Fig. 8 and Fig. 9 show overall results obtained both from the visualization and from CTA. The experimental data are compared to the results by Trávníček et al. [3] and Williamson [9]. Results of the Strouhal number correlations (5) and (11) are also shown for comparison. Fig. 8 shows the St–Re relationship, while in Fig. 9 the concept of the effective temperature and the effective Reynolds number is applied, i.e. the St-Re_{eff} relationship is shown. In an ideal case, the measured data points should lie on a curve of the same color in Fig. 8. However as can be seen both in Fig. 8 and Fig. 9, the new experimental results obtained both from the visualization and CTA lie by considerably lower

Tab. 1. Results from the visualization measurement; a – upper cooled cylinder, b – reference isothermal cylinder.

#	U $(m \cdot s^{-1})$	T_w (K)	T_∞ (K)	T^*	T_{eff} (K)	ν_∞ $(m^2 \cdot s^{-1})$	Re	ν_{eff} $(m^2 \cdot s^{-1})$	Re_{eff}	f (Hz)	St
1a	0.622	310.7	310.7	1.00	310.7	$1.762 \cdot 10^{-5}$	70.39	$1.762 \cdot 10^{-5}$	70.39	35.85	0.1156
1b	0.642	310.7	310.7	1.00	310.7	$1.762 \cdot 10^{-5}$	72.66	$1.762 \cdot 10^{-5}$	72.66	35.63	0.1113
2a	0.622	309.8	309.8	1.00	309.8	$1.752 \cdot 10^{-5}$	70.76	$1.753 \cdot 10^{-5}$	70.76	35.40	0.1142
2b	0.642	301.2	309.8	0.97	307.4	$1.752 \cdot 10^{-5}$	73.04	$1.728 \cdot 10^{-5}$	74.07	35.78	0.1118
3a	0.622	311.4	311.4	1.00	311.4	$1.768 \cdot 10^{-5}$	70.12	$1.768 \cdot 10^{-5}$	70.12	35.90	0.1061
3b	0.642	291.15	311.4	0.93	305.7	$1.768 \cdot 10^{-5}$	72.39	$1.712 \cdot 10^{-5}$	74.79	36.77	0.1149
4a	0.622	309.1	309.1	1.00	309.1	$1.745 \cdot 10^{-5}$	71.07	$1.745 \cdot 10^{-5}$	71.07	34.50	0.1113
4b	0.642	281.2	309.1	0.91	301.2	$1.745 \cdot 10^{-5}$	73.37	$1.667 \cdot 10^{-5}$	76.78	36.33	0.1135

Tab. 2. Results from the CTA measurement; a – upper cooled cylinder, b – reference isothermal cylinder

#	U $(m \cdot s^{-1})$	T_w (K)	T_∞ (K)	T^*	T_{eff} (K)	ν_∞ $(m^2 \cdot s^{-1})$	Re	ν_{eff} $(m^2 \cdot s^{-1})$	Re_{eff}	f (Hz)	St
1a	0.642	281.2	311.7	0.90	303.1	$1.771 \cdot 10^{-5}$	72.49	$1.686 \cdot 10^{-5}$	76.16	36.62	0.1141
2a	0.642	281.2	311.8	0.90	303.2	$1.773 \cdot 10^{-5}$	72.42	$1.687 \cdot 10^{-5}$	76.11	37.84	0.1179
3a	0.642	281.2	311.8	0.90	303.2	$1.772 \cdot 10^{-5}$	72.43	$1.687 \cdot 10^{-5}$	76.11	37.84	0.1179
1b	0.622	311.1	311.1	1.00	311.1	$1.766 \cdot 10^{-5}$	70.50	$1.766 \cdot 10^{-5}$	70.50	37.84	0.1216
2b	0.622	311.2	311.2	1.00	311.2	$1.766 \cdot 10^{-5}$	70.49	$1.766 \cdot 10^{-5}$	70.49	37.84	0.1216
3b	0.622	311.2	311.2	1.00	311.2	$1.766 \cdot 10^{-5}$	70.50	$1.766 \cdot 10^{-5}$	70.50	39.06	0.1255

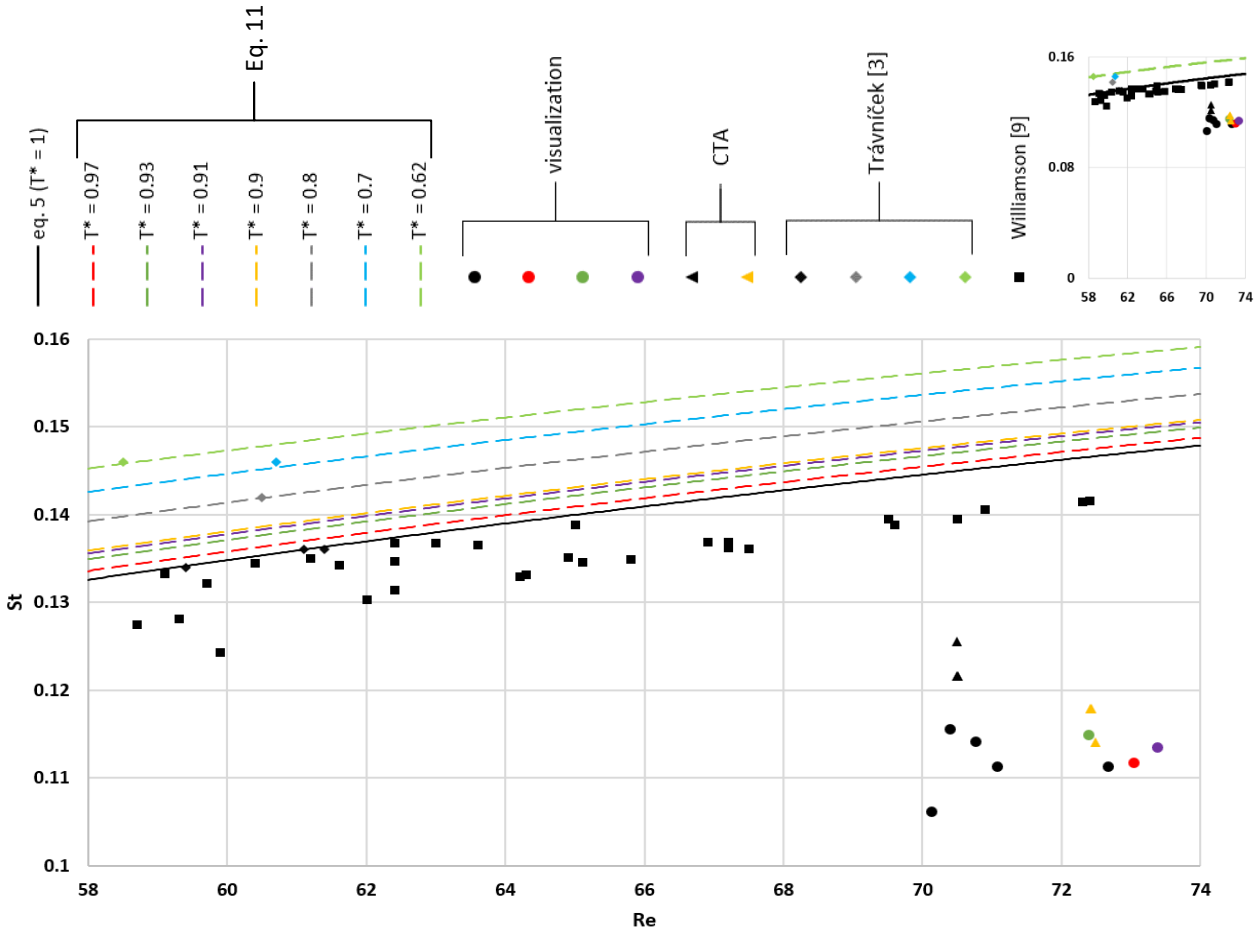

Fig. 8 Dependence of the Strouhal number St on the Reynolds number Re.

Strouhal numbers that the theoretical values (curves) and the literature data by Trávníček et al. [3] and Williamson [9]. The deviations of Strouhal number is in the range from 20.2 to 26.6 % for the visualization method and from 13.4 to 23.7 % for CTA. Literature data by Williamson show a maximum deviation of 7.7 % (mean deviation is around 2.7 %) and the data by Trávníček et al. differ by less than 1 %. The measured flow velocity deviated from equation (9) by 14.6 ÷ 17.3 % in case of CTA. These considerable differences are suspected to be caused by an unsteady character of the flow with relatively high turbulence intensity. A potential rising flow coming from the heater at the channel inlet could occur close to measurement area. The turbulence intensity was estimated to lie in the range from 8.1 to 14.6 %. In the region close to the cylinders the turbulence intensity could be of around 8 to 9 %.

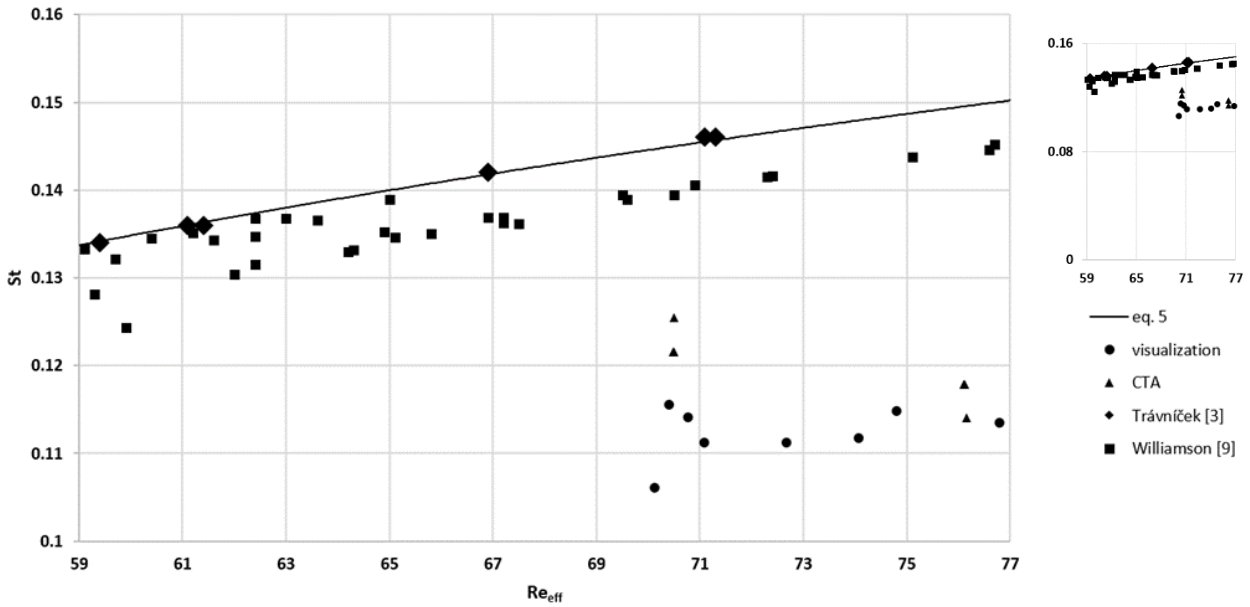

Fig. 9 Dependence of the Strouhal number St on the effective Reynolds number Re_{eff}.

5 Conclusion

An experimental channel intended for investigation of a wake behind a cooled cylinder was designed and constructed. The channel was used at temperatures up to 313 K and flow velocities from 0.62 to 0.64 m · s^{-1}. The channel was equipped with two cylinders. Temperature of one cylinder was varied by employing water cooling. The wall temperature was set to $T_W = T_\infty$ (isothermal case), T_W = 301.1 K, T_W = 291.1 K a T_W = 281.1 K. The second cylinder was used as a reference as its temperature was kept constant equal to the air flow temperature $T_W = T_\infty$. The flow characteristics were studied using the visualization technique with a fog generator. The flow velocity and the vortex shedding frequency were determined using the constant temperature anemometry.

The experimental setup was found to be suitable for the air-flow visualization. The preliminary measurements confirmed influence of the cylinder cooling on the wake character. However, the collected data showed a considerable deviation from the theoretical values for the Strouhal number of up to 26.6 % at the given Reynolds number. Current design of the channel was found to be inconvenient for an accurate measurement of characteristic magnitudes of a body flow. Modifications of the channel design, such as improvement of the front heater, employment of thermal insulation on outer walls of the channel, or installation of a flow stabilization element at the inlet are planned in order to improve the flow performance, especially at the inlet section.

Acknowledgment

This research was carried out at the Technical University of Liberec as part of the project "Experimental, theoretical and numerical research in fluid mechanics and thermomechanics, no. 21291“ with the support of the Specific University Research Grant, as provided by the Ministry of Education, Youth and Sports of the Czech Republic in the year 2019 and with the institutional support RVO: 61388998.

References

1. R. Munson, T. H. Okiishi, W. W. Huebsch, A. P. Rothmayer, *Fundamental of Fluid Mechanics* (Wiley, 2012)
2. J. Pulec, *master's degree thesis* (TU Liberec, 2018)
3. Z. Trávníček, A.-B. Wang, W.-Y. Tu, Exp Fluids **55**, 1679 (2014)
4. J. C. Lecordier, L. Hamma, P. Paranthoën, Experiments in Fluids **10**, 224 (1991)
5. J. C. Lecordier, F. Dumouchel, P. Paranthoën, International Journal of Heat and Mass Transfer **42,** 3131 (1999)
6. J. C. Lecordier, L. W. B. Browne, Le S. Masson, F. Dumouchel, P. Paranthoën, Experimental Thermal and Fluid Science **21**, 227 (2000)
7. A.-B. Wang, Z. Trávníček, K. C. Chia, Physics of Fluids **12**, 1401 (2000)
8. R. J. Goldstein, H. H. Cho, Experimental Thermal and Fluid Science **10**, 416 (1995)
9. C. H. K. Williamson, Journal of Fluid Mechanics **206**, 579 (1989)